Investigation of the compression of high-aspect targets irradiated with a laser pulse of the second harmonic of the "Iskra-4" iodine laser

S. A. Bel'kov, A. V. Bessarab, I. N. Voronich, S. G. Garanin, G. V. Dolgoleva, A. I. Zaretskiĭ, V. M. Izgorodin, B. N. Ilyushechkin, G. G. Kochemasov, A. V. Kunin, S. P. Martynenko, S. G. Merkulov, N. N. Rukavishnikov, A. V. Ryadov, N. A. Suslov, and S. A. Sukharev

(Submitted 3 July 1991; resubmitted 11 September 1991)
Zh. Eksp. Teor. Fiz. **101**, 80–88 (January 1992)

Theoretical modeling of experiments on the compression of targets under "exploding pusher" shell conditions, carried out at the "Iskra-4" facility with the iodine laser pulsed at its fundamental frequency ($\lambda = 1.315\,\mu$m) showed a correlation between the increase in the discrepancy between the calculated and experimental neutron yields and increase of the aspect ratio of the shell of the target used in the experiment. After conversion of the "Iskra-4" facility to generate the second harmonic and improving the beam uniformity in the region of the target, a series of experiments was carried out on the compression of high-aspect targets $A_S > 300$. In this series a record neutron yield for this installation, $N = 6\times 10^7$, was obtained in experiments with glass-shell targets.

1. INTRODUCTION

Experiments have recently been carried out at the most powerful foreign facilities designed to study laser thermonuclear fusion (LTF), on the heating and compression of DT (or D_2) in gas-filled glass shell targets with large ratio of radius R_0 to thickness ΔR of the target $A_S = R_0/\Delta R \simeq 300$–$600$.[1-4]

For such values of A_S the maximum efficiency in transforming the absorbed energy into internal energy of DT occurs for an irradiating wavelength $\lambda = 0.35$–$0.53\,\mu$m. In addition, large aspect ratios A_S enable the shell to be accelerated to high velocities $V_{sh} \sim (A_S P_a/\rho_{sh})^{1/2}$, where P_a is the ablation pressure, ρ_{sh} is the density of the shell material. As a result, a strong shock wave is formed in the DT gas which, on focusing and reflection from the center, heats the thermonuclear fuel to high temperatures. For example, in experiments with such targets at facilities such as "Nova" (USA, $E_L \sim 20$ kJ, $\lambda = 0.35\,\mu$m, $\tau_L \sim 1$ ns),[1] "Gekko-XII" (Japan, $E_L = 10$ kJ, $\lambda = 0.53\,\mu$m. $\tau_L \sim 0.7$ ns),[3] and "Omega" (USA, $E_L \sim 2$ kJ, $\lambda = 0.35\,\mu$m, $\tau_L \sim 1$ ns)[2] neutron yields for the DT reaction were $N \sim 2\times 10^{13}$, $\sim 10^{13}$, $\sim 6\times 10^{11}$ respectively. At the "Vulcan" installation (UK, $E_L = 800$ J, $\lambda = 0.53\,\mu$m, $\tau_L \sim 0.8$ ns)[4] the neutron yield in the DD reaction was at the $N \sim 10^8$ level.

In fact, irradiation of high-aspect-ratio shells is the main method for obtaining high-temperature plasmas (ion temperature $T_i \gtrsim 10$ keV) and generating neutrons using short-wavelength ($\lambda \lesssim 0.53\,\mu$m) laser radiation. In view of the small values of density on implosion of high-aspect shells ($\rho_f < 1$ g/cm^3), such targets cannot be brought up to thermonuclear burn conditions for laser radiation energy $E_L \lesssim 1$ MJ. The interest in this type of target is therefore connected with a study of the features of the compression of super-thin shells, the development of diagnostic methods for the plasma and the use of generated α-particles for various purposes, including studying the Rayleigh-Taylor instability.[5]

The initial results of experiments on irradiating high-aspect targets with second harmonic radiation of an iodine laser ($\lambda = 0.657\,\mu$m) at the "Iskra-4" facility are given in the present work.

It should be pointed out that on increasing the wavelength the optimum (from the point of view of maximizing the hydrodynamic efficiency) value of A_S increases, and according to calculation is $A_S \gtrsim 550$. A key feature of the work was the improvement in the uniformity of irradiation of the target by using random phase plates, changing the local wavefront of the second harmonic radiation randomly.

In addition, results are given in a systematic form of earlier studies on generating DT neutrons at a wavelength $\lambda = 1.315\,\mu$m.

2. EXPERIMENTAL ARRANGEMENT

A regime close to "exploding pusher" shell conditions was earlier studied in detail at the Iskra-4 facility[6,7] which is a single-channel iodine laser (operating wavelength of the radiation $\lambda_0 = 1.315\,\mu$m). Previously this was studied experimentally, in particular the conditions close to the "explosive" shell.[8] In these experiments gas-filled targets ($P_{DT} \simeq 10$–30 atm) with moderate aspect ratios $A_S \simeq 20$–100 were irradiated with four beams situated in tetrahedral geometry. The total energy of the laser radiation

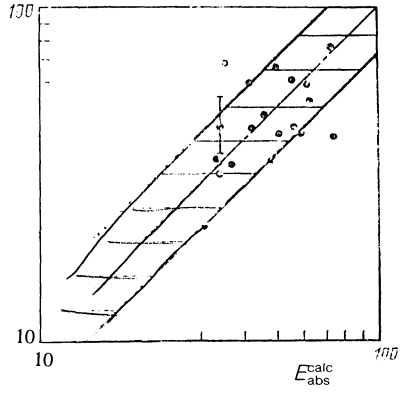

FIG. 1. Comparison of calculated and experimental values of the absorbed energy E_{abs} in experiments on irradiating spherical glass microtargets at the "Iskra-4" facility.

 0038-5646/92/010043-05$05.00

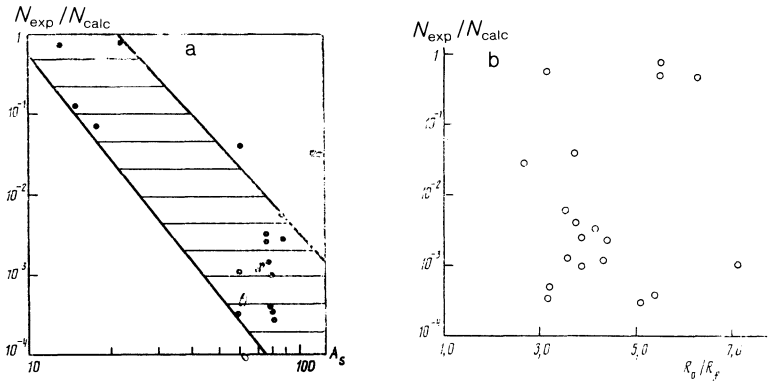

FIG. 2. Dependence of the ratio of experimental and calculated neutron yields N_{exp}/N_{calc}, for experiments represented in Fig. 1, on the aspect ratio A_S (a) of the target shell, and also on the calculated R_0/R_f degree (b).

injected into the target chamber varied within the limits $E_L \simeq 300$–500 J, for a laser pulse duration at half height $\tau_{0.5} \simeq 0.2$–0.3 ns. The absorption coefficient k_{abs} in this mode of irradiating the targets did not exceed the value $k_{abs} \lesssim 10$–15%. The yield of thermonuclear neutrons $N \lesssim (2\text{–}3) \times 10^6$.

The theoretical modeling of the experiments carried out on the one-dimensional hydrodynamic SNDP program[9] showed satisfactory agreement between calculated and experimental values of the energy absorption E_{abs} (Fig. 1). In the calculations account was taken of:

1) the experimental conditions for directing the laser beam onto the target, namely: the longitudinal displacement Δz of the center of the target relative to the focus of the parabolic mirror, aiming the radiation onto the target, the angular error in the beam axis relative to the target center, the divergence of the laser radiation, etc;

2) the processes: inverse bremsstrahlung and resonance absorption of the laser radiation, the generation of "hot" electrons and the acceleration of "fast" ions;

3) the effect of the increase in the steepness of the density profile in the region of the critical surface, due to the pressure of the laser radiation;

4) the processes: electron and ion thermal conductivity with a limiting flux (flux limiter $f = 0.5$), electron-ion relaxation, transfer of x-ray radiation in a single-group diffusion approximation.

Comparison of the experimental N_{exp} and calculated N_{calc} neutron yields shows the existence of a certain correlation between the increase in the difference between N_{exp} and N_{calc} and the growth of the target aspect ratio A_S (Fig. 2a). For $A_S \simeq 100$ this difference reaches $N_{calc}/N_{exp} \sim 10^3$. Note that this difference between the experimental and calculated neutron yields is in no way connected with the irradiation symmetry, which was low in the experiments considered here. This is clear from Fig. 2b, where N_{exp}/N_{calc} is plotted against the calculated radial compression R_0/R_f. No correlation whatever is observed between the point positions on this figure.

After modernizing the installation and conversion to irradiating targets with the pulsed second harmonic[10] ($\lambda_{2\omega} = 0.657$ μm) with parameters in the target chamber $E_{2\omega} \simeq 200$–300 J and $\tau_{0.5} \simeq 0.25$–0.6 ns, the absorption coefficient of the laser radiation increased by a factor 2–2.5 and was $k_{abs} \simeq 0.3$–0.5. Under these conditions, in spite of the fact that the wavelength of the second harmonic radiation of the iodine laser considerably exceeds that of the foreign facilities mentioned above, the compression conditions for high-

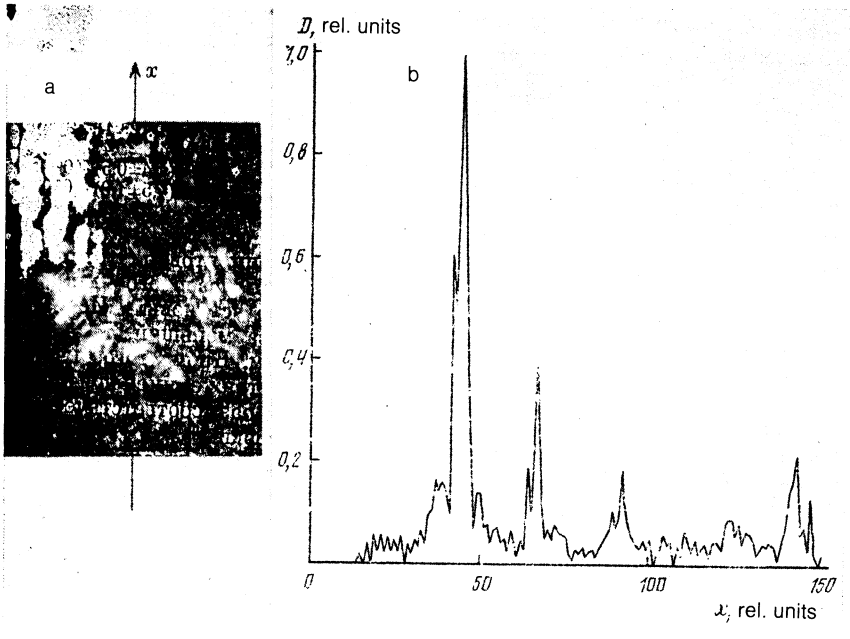

FIG. 3. Photorecorded (a) and densitometer (b) distributions of energy density of laser illumination in the beam cross section without phase plates after the mosaic frequency converter.

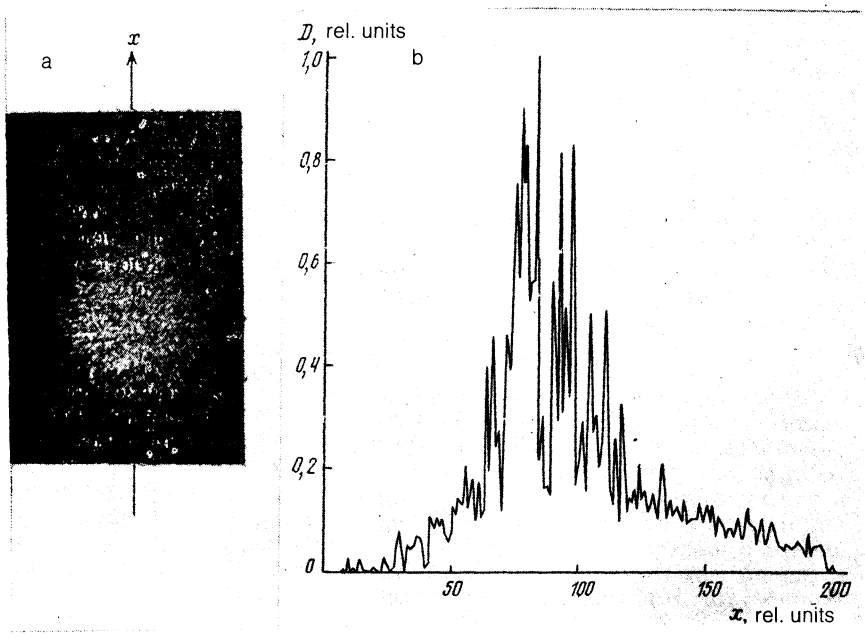

FIG. 4. Photorecorded (a) and densitometer (b) distributions of energy density of laser illumination in the same cross section as in Fig. 3 after the use of phase plates.

aspect targets could be attempted. In fact, simple estimates on the assumption of hydrodynamic similarity of the compression of high-aspect shells show that a target with $A_S = 450$, $R_0 = 0.6$ mm, $\Delta R = 1.3$ μm is optimal, giving under the experimental conditions in the Gekko-XII installation a maximum neutron yield for a laser pulse $E_L \approx 10$ kJ, $\tau_L \approx 1$ ns (Ref. 2), scaled to the energy of "Iskra-4" should have a radius $\xi = (E_{\text{Gekko}}/\tau_{\text{Iskra}})^{1/3} \approx 3.2$ times less, i.e., $R_0 \approx 190\,\mu$m and correspondingly a thickness $\Delta R = 0.4\,\mu$m. In addition, to preserve the hydrodynamic similarity it is also necessary to reduce by ξ fold the pulse duration to $\tau_L = 0.3$ ns, which just corresponds to the characteristic pulse length of the laser's output.

The change to irradiating the target with second harmonic radiation advanced to foremost position the question of the spatial structure of the beam in the focal region of the parabolic focusing mirror. A typical photorecording of the energy density distribution of the laser radiation in the beam cross-section at a distance $\Delta z = -107$ μm from the minimum focus spot is shown in Fig. 3 (the minus sign corresponds to a displacement of the recorded section into the pre-focal region). Overall, both the mosaic structure of the frequency converter[10] situated at the beam exit and the near-field structure of the near-field beam itself are clearly apparent. In conjunction with the small number of beams, such irradiation distributions on the target surface give rise to both large-scale (characteristic dimensions $l \sim R_0$) and small-scale ($l \sim 10$–$20\,\mu$m) non-uniformity of illumination, with intensity minima close to zero.

To obtain a bell-shaped intensity distribution in the region of the positioning of the target, a beam homogenizer introducing random distorions of the wave-front was used.[11,12] An image of the spatial structure of the beam obtained by using the present method is shown in Fig. 4 at the same section of the beam before focus as in Fig. 3. The characteristic scale of the nonuniformity, as a result of the measures adopted, was reduced to the dimension determined by the diffraction limit and amounted to $l \sim 1$–2 μm in the region of the target position. The envelope of the illumination energy density distribution then has a form close to Gaussian with an angular divergence, containing 80% of the beam energy, of $\theta_{0.8} = (3\text{–}4) \times 10^{-4}$ rad.

3. EXPERIMENTAL RESULTS

A series of 7 experiments on the irradiation of high-aspect shells was carried out under the conditions described above (see Table I). The aspect ratio varied from $A_S \approx 200$ to $A_S \approx 380$ and the DT gas pressure was equal to $P_{\text{DT}} \sim 4$ atm. The laser radiation energy fed into the reaction chamber varied over the range $E_{2\omega} \approx 120$–250 J for a pulse duration $\tau_{0.5} = 0.26$–0.6 ns. The energy absorption measured with ca-

TABLE I. Target parameters and results of the measurements of laser impulse parameters and neutron yield in experiments at "Iskra-4" equipment.

№	ϕ_T, μm	A_S	$E_{2\omega}$, J	$\tau_{0.5}$, ns	N
1	378	378	206	0,6	$(8{,}5\pm1{,}4)\cdot10^6$
2	392	327	220	0,47	$(5{,}8\pm1{,}4)\cdot10^7$
3	312	240	110	0,3	$(3{,}5\pm1{,}2)\cdot10^6$
4	355	237	146	0,62	$(2\pm1)\cdot10^5$
5	316	211	198	0,3	$(4{,}8\pm1{,}4)\cdot10^6$
6	315	210	211	0,25	$(1{,}4\pm0{,}5)\cdot10^6$
7	340	200	196	0,55	$(4{,}5\pm1{,}3)\cdot10^6$

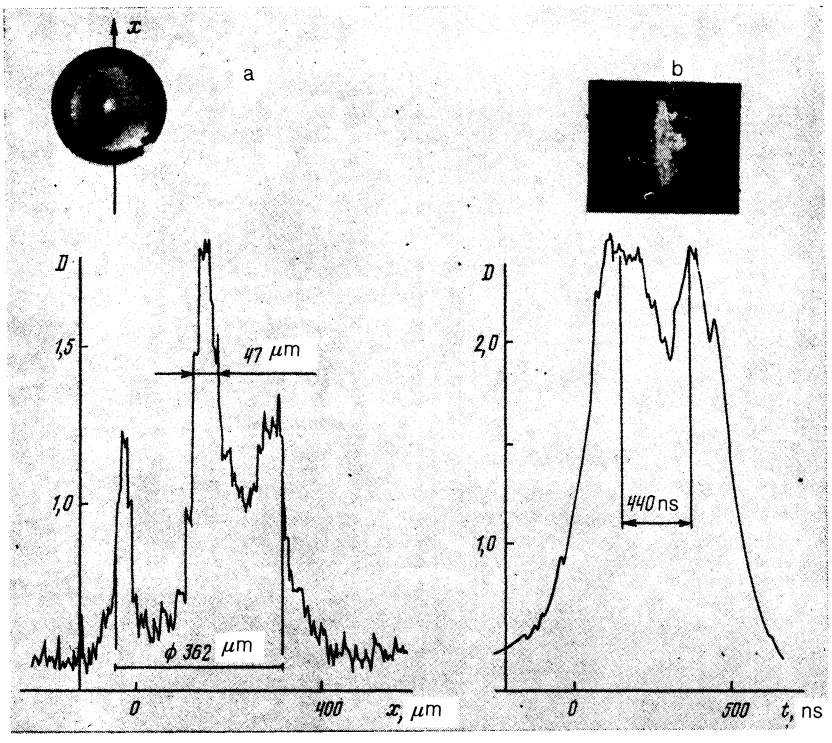

FIG. 5. Recorded plasma luminosity in the x-ray radiation obtained using (a) a pinhole camera and (b) x-ray streak camera.

lorimeters (type $4-x$) at different points in the reaction chamber was $E_{abs} \simeq 40$–150 J, corresponds to an absorption coefficient $k_{abs} \simeq 0.35$–0.65.

The longitudinal displacement of the target along the laser beam axis relative to the minimum focal spot varied from $\Delta z = -90\,\mu$m (uniform illumination of the target) to $\Delta z = +155\,\mu$m (sharp focusing of the illumination onto the target surface). In all experiments the recorded neutron yield was $N \simeq 2\times 10^5$–6×10^7. The best results (among them also the record for "Iskra-4" in experiments on irradiating spherical targets, a neutron yield $N \simeq 6\times 10^7$) were obtained under conditions of focusing beams onto the center of the target (longitudinal shift $\Delta z = 0$).

It should be noted that for a displacement $\Delta z = 0$ there is no overlap of the beams onto the target surface and the illumination of the target is characterized by strong large-scale nonuniformity, easily seen on pinhole camera photographs of luminosity of the plasma. A typical pinhole-camera picture of a target is shown in Fig. 5a, a recorded in one of the experiments beyond an Al filter $d = 8\,\mu$m thick. The nonuniform luminous corona and the central compressed nucleus are clearly seen. The fact that the central nucleus corresponds to the moment of compression follows from the recording of the time-resolved plasma luminosity, obtained with an x-ray streak camera in the same experiment (Fig. 5b). The luminosity of the corona and the central nucleus take place at different moments in time and the delay in the emission from the nucleus $\Delta t = 0.44$ ns corresponds to the velocity of the shell $V_{sh} \simeq 4\times 10^7$ cm/s, which agrees satisfactorily with the calculated values of the shell velocity.

The maximum neutron yield $N = 6\times 10^7$ was obtained in an experiment with target diameter $\phi_T = 392\,\mu$m, $\Delta R = 0.6\,\mu$m, $A_S = 327$, $P_{DT} = 3$ atm and laser pulse $E_{2\omega} = 220$ J, $\tau_{0.5} = 0.47$ ns. The energy absorption was $E_{abs} \lesssim 150$ J and strong anisotropy in the spread of the plasma was observed. On the pinhole-camera pictures taken in different directions (Fig. 6) the central luminous region of involved shape is clearly visible, having the form of different projections of a tetrahedron. On the whole, these projections agree satisfactorily with the geometry of the target illumination and the direction of observation of the pinhole camera.

In a hydrodynamic calculation carried out with the SNDP program, taking account of the electron thermal flux (flux limiter $f = 0.03$) it was found that the calculated value of the absorbed energy agrees well with that measured experimentally $E_{abs}^{calc} = 134$ J, while the calculated neutron yield $N_{calc} = 1.5\times 10^{10}$ is about 260 times greater than the experimental value. The calculated time dependence of the neutron yield is shown in Fig. 7. It is seen from the calculation that the neutron generation takes place in two stages: up to approximately $N \sim 10^8$ neutrons are generated in the first shock wave (the moment of arrival of the shock wave center at the DT gas-glass interface corresponds to the time $t_2 = 1.11$ ns) and then an adiabatic final compression of the DT gas takes place, as a result of which the neutron yield grows to $N_{calc} = 1.5\times 10^{10}$. If it is assumed that as a result of

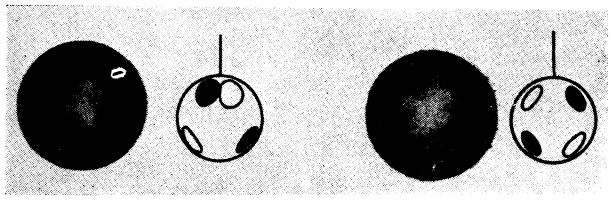

FIG. 6. Recorded plasma luminosity in the x-ray radiation obtained using a pinhole camera with different orientations relative to the laser beams illuminating the target in the experiment with the record neutron yield. The visible illumination spot is shown by the dense oval.

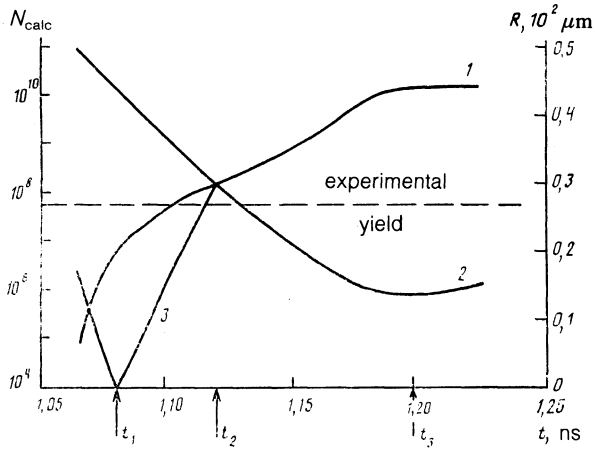

FIG. 7. (1) Generation of neutron yield, (2) trajectory of the motion of the DT gas–glass boundary, and (3) shock wave front in the calculation modeling the experimental conditions for the record neutron yield. t_1—the time of focusing the shock wave at the center; t_2—the time for the reflected shock wave to emerge at the gas–glass boundary; t_3—the time for the maximum compression of the target.

mixing which occurs after the emergence of the shock wave at the contact boundary the calculated final compression stage does not exist, then the neutron yield at the time t_2 agrees satisfactorily with experiment. On the other hand, it follows from the present calculation that the target parameters for the conditions of the experiment are not optimal, since the main neutron yield corresponds to the final compression stage.

4. CONCLUSIONS

As a result of the experimental investigations carried out, the possibility in principle of realizing the heating of DT gas has been shown and the stable generation of neutrons in a strongly convergent shock wave which is formed on compression of high-aspect targets ($A_S \gtrsim 300$) irradiated with a laser pulse of wavelength $\lambda = 0.657\,\mu$m under the conditions in "Iskra-4." This is an appreciably greater wavelength region of illumination than that studied earlier in other installations for LTF. The use of phase plates introducing random distortions in the structure of the wave-front of the "Iskra-4" illumination made it possible to improve qualitatively the intensity of the beam focus, which also allowed, finally, the experiments described above to be carried out. In the experiments record neutron yields for "Iskra-4" were recorded in targets of direct illumination. Comparison of the experimental results with their calculated modeling in the SNDP hydrodynamic method allowed us to conclude that the parameters obtained in this series of experiments are not the limiting values for this installation.

[1] M. D. Cable, S. G. Prussin, S. G. Glendenning *et al.*, Laser Program Annual Report UCRL-50021-86 (1986).
[2] M. C. Richardson, P. W. McKenty, R. L. Keck, F. J. Marshall, D. M. Roback, C. P. Verdon, R. L. McCrory, J. M. Soures, and S. M. Lane, Phys. Rev. Lett. **56**, 2048 (1986).
[3] H. Takabe, M. Yamanaka, K. Mima, C. Yamanaka, H. Azechi, N. Miyanaga, M. Nakatsuka, T. Jitsuno, T. Norimatsu, M. Takagi, H. Nishimura, M. Nakai, T. Yabe, T. Sasaki, K. Yoshida, K. Nishihara, Y. Kato, Y. Izawa, T. Yamanaka, and S. Nakai, Phys. Fluids **31**, 2884 (1988).
[4] A. P. Fews, M. J. Lamb, M. Savage *et al.*, Annual Report, Central Laser Facility, Rutherford-Appleton Laboratory, RAL-90-026, p. 33 (1990).
[5] A. P. Fews, M. J. Lamb, M. Savage, *et al.* Annual Report, Central Laser Facility, Rutherford-Appleton Laboratory, RAL-90-026, p. 31 (1990).
[6] S. B. Kormer, Izv. Akad. Nauk SSSR Ser. Fiz. **44**, 2002 (1980).
[7] A. I. Zaretskiĭ, G. A. Kirillov, S. B. Kormer G. G. Kochemasov, V. M. Murugov, and S. A. Sukharov, Izv. Akad. Nauk SSSR Ser. Fiz. **48**, 1611 (1984).
[8] S. A. Bel'kov, A. V. Bessarab, A. V. Veselov, S. G. Garanin, G. V. Dolgoleva, A. I. Zaretskiĭ, G. A. Kirillov, G. G. Kochemasov, N. V. Maslov, I. N. Nikitin, S. I. Petrov, A. V. Ryadov, A. V. Senik, N. A. Suslov, and S. A. Sukharev, Zh. Eksp. Teor. Fiz. **97**, 834 (1990) [Sov. Phys. JETP **70**(3), 467 (1990)].
[9] S. A. Bel'kov, S. N. Gaĭduk, S. G. Garanin, G. V. Dolgoleva, and G. G. Kochemasov, Vopr. At. Nauki Tekh. Ser. Matemat. Model. Fiz. Prots. **1**, 76 (1990).
[10] I. N. Voronich, D. G. Efimov, A. I. Zaretskiĭ, G. A. Kirillov, E. G. Kosyak, G. G. Kochemasov, S. G. Merkulov, N. N. Rukavishnikov, A. V. Ryadov, V. A. Samylin, S. V. Sokolovskiĭ, and S. A. Sukharev, Izv. Akad. Nauk. SSSR Ser. Fiz. **54**, 2024 (1990).
[11] Y. Kato and K. Mima, Appl. Phys. **B29**, 186 (1982).
[12] Y. Kato, K. Mima, N. Miyanaga, S. Arinaga, Y. Kitagawa, M. Nakatsuka, and C. Yamanaka, Phys. Rev. Lett. **53**, 1057 (1984).

Translated by R. Berman